Available online at www.sciencedirect.com
ScienceDirect
Ceramics International 33 (2007) 1509–1513
CERAMICS INTERNATIONAL
www.elsevier.com/locate/ceramint

Fabrication and magnetic properties of cobalt-dispersed-alumina composites

Xiaomei Shi [a,b], Yubai Pan [a,*], Jingkun Guo [a]

[a] State Key Lab of High Performance Ceramics and Superfine Microstructure, Shanghai Institute of Ceramics, Chinese Academy of Sciences, 1295 Ding Xi Road, Shanghai 200050, PR China
[b] Graduate School of the Chinese Academy of Sciences, Beijing, PR China

Received 2 March 2006; received in revised form 28 March 2006; accepted 18 May 2006
Available online 20 September 2006

Abstract

High-density cobalt-dispersed-alumina (Co/Al_2O_3) composites were successfully prepared by hot-pressing of alumina-cobalt composite powders with fine cobalt ~30 nm in diameter. The nanocomposite powders were prepared by co-deposited processing of $Al^{3+}$and Co^{2+}, followed by calcination and selective reduction. The phase composition of Co/Al_2O_3 composites were α-Al_2O_3, fcc-Co and a little amount of hcp-Co. Microstructural investigations revealed that submicron-sized cobalt particles were dispersed homogeneously at alumina grain boundaries, forming intergranular composites. Meanwhile growth and coalescence of cobalt particles occurred with increasing Co-content. The ferromagnetic properties of the composites were measured, because of the magnetic dispersions, which indicated a functional value of Co/Al_2O_3 composites. The effects of grain size and the residual stresses on magnetic properties for Co/Al_2O_3 system were discussed in detail.

Keywords: A. Hot-pressing; B. Grain size; C. Magnetic properties; Microstructure

1. Introduction

Alumina is one of the most widely used structural ceramic materials for its physical properties and chemical stability. However, the applications of alumina are limited by its brittleness. Al_2O_3-matrix composite ceramics have been widely explored in the last decade [1]. Much work is focus on improving mechanical properties of Al_2O_3 ceramics by incorporating the submicron or nanometer sized metal [2–7] or ceramic second particles [8,9]. In addition, the excellent functionalities in Al_2O_3-metal systems have attracted much attention in the recent years [10–13]. Considering the magnetic properties of Co/Al_2O_3 composites, it is expected that the ferromagnetism of cobalt will be demonstrated by dispersing fine cobalt particles in Al_2O_3 matrix. For practical uses of small magnetic particles, a high saturation magnetization and coercivity are required [14]. Magnetic properties of cobalt can meet the practical requirement. Moreover, significant improvement in mechanical properties in Co/Al_2O_3 system was achieved by incorporating submicron-sized Co into the Al_2O_3 matrix [6]. The present work addressed a successful procedure to obtain Co/Al_2O_3 composite ceramics that possess desirable microstructure and magnetic properties.

Dense Co/Al_2O_3 composites were fabricated through calcination, reduction and hot-pressing processes to the precursor of Co/Al_2O_3 composite powders prepared by co-deposition method. By the solution chemistry route, we obtained the controlled microstructure, in which the second phase had a fine and homogeneous dispersion. In the present work, the preparation process and microstructural characteristic were investigated. Moreover, the effect of Co-content and the residual stresses on the magnetic properties of the Co/Al_2O_3 composites was discussed.

2. Experimental procedure

Co/Al_2O_3 nanocomposite powders were prepared by co-precipitation. Precipitation was carried out from aqueous solution of metal nitrates: $Al(NO_3)_3{\cdot}9H_2O$ (Analytical Pure) and $Co(NO_3)_2{\cdot}6H_2O$ (Analytical Pure) in known proportions at room temperature. Aqueous NH_4HCO_3 (Analytical Pure) was used as a precipitation agent for synthesis of Co/Al_2O_3. To decrease the degree of the aggregation, polyethylene glycol

* Corresponding author. Tel.: +86 21 52412820; fax: +86 21 52413903.
E-mail address: ybpan@mail.sic.ac.cn (Y. Pan).

0272-8842/$32.00
doi:10.1016/j.ceramint.2006.05.017

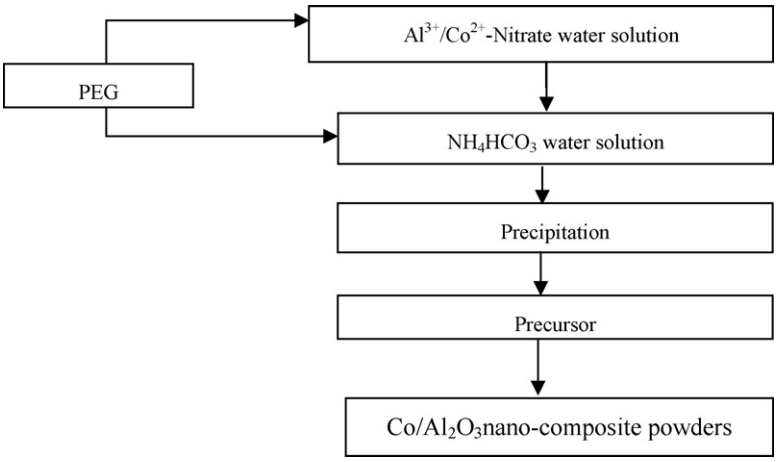

Fig. 1. Flowchart for the preparation of Co/Al_2O_3 nanocomposite powders.

(PEG) was added as dispersant in the processing. The general fabrication routes for Co/Al_2O_3 composites are illustrated by the flow diagram in Fig. 1. The mixed Al^{3+}/Co^{2+}-nitrate water solution was added dropwise to NH_4HCO_3 water solution under vigorous stirring. Its reactions were given by the following equations [15],

$$3Al^{3+} + 9HCO_3^- + H_2O \rightarrow Al_2(CO_3)_3{\cdot}Al(OH)_3{\cdot}4H_2O\downarrow + 6CO_2\uparrow \quad (1)$$

$$3Co^{2+} + 6HCO_3^- + H_2O \rightarrow Co(CO_3)_2{\cdot}2Co(OH)_2{\cdot}2H_2O\downarrow + 5CO_2\uparrow \quad (2)$$

The precipitates were not dissolved in OH^- solution [16]. To ensure complete reaction, an excess of NH_4HCO_3 was used and pH value of the mixed solution was between 8 and 9 during precipitation. The resulting precipitates were washed, filtered and dried at 110 °C for 24 h. The as-dried precipitates were calcined, and then the as-calcined powders were in situ selectively reduced at 950 °C for 2 h in H_2. Finally Co/Al_2O_3 nanocomposite powders were obtained, with an average size of 30 nm. Co/Al_2O_3 composites were prepared by hot-pressing at 1400 °C in Ar atmosphere under the pressure of 30 MPa for 30 min.

Phase compositions were identified by X-ray diffraction (XRD; Rigaku, Tokyo, Japan) analysis. The microstructure was characterized by scanning electron microscopy (SEM; JSM-6700F, JEOL, Japan) and the transmission electron microscopy (TEM; JEM-200CX, Japan) The magnetic properties were tested using vibrating sample magnetometer (VSM; model 155, EG&G Princeton. Research, USA) with an applied magnetic field up to ±10 kOe at room temperature.

3. Results and discussion

3.1. Formation and microstructure of Co/Al_2O_3 composites

The XRD patterns for the Co/Al_2O_3 composite are shown in Figs. 2 and 3. After calcining at 850 °C, only the peaks for

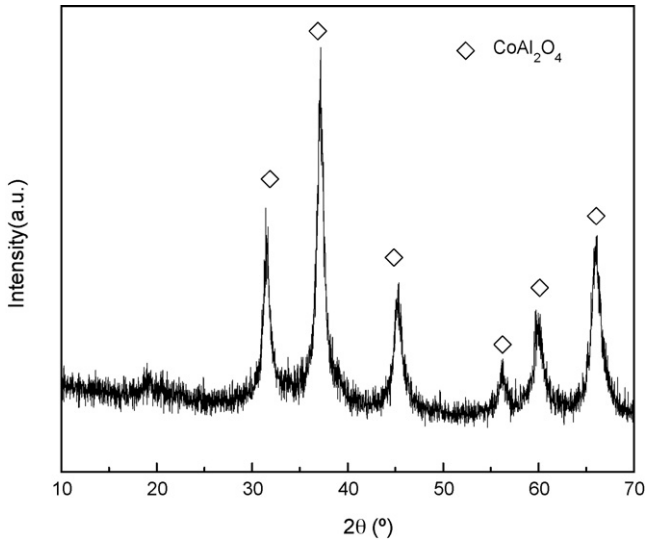

Fig. 2. XRD patterns for the calcined powders of 15 vol.% Co/Al_2O_3 (850 °C, in Air).

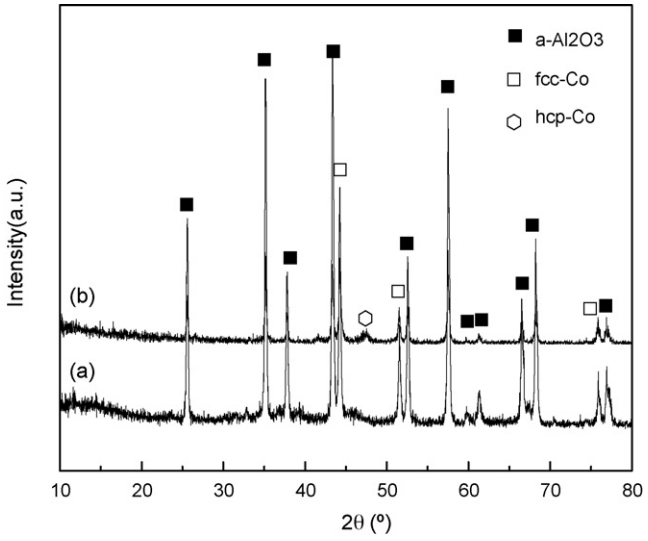

Fig. 3. XRD patterns for the 15 vol.% Co/Al_2O_3 at the different stages of processes (a) the reduced powders (at 950 °C in H_2) and (b) the 15 vol.% Co/Al_2O_3 composites (hot-pressed at 1400 °C under 30 MPa for 30 min).

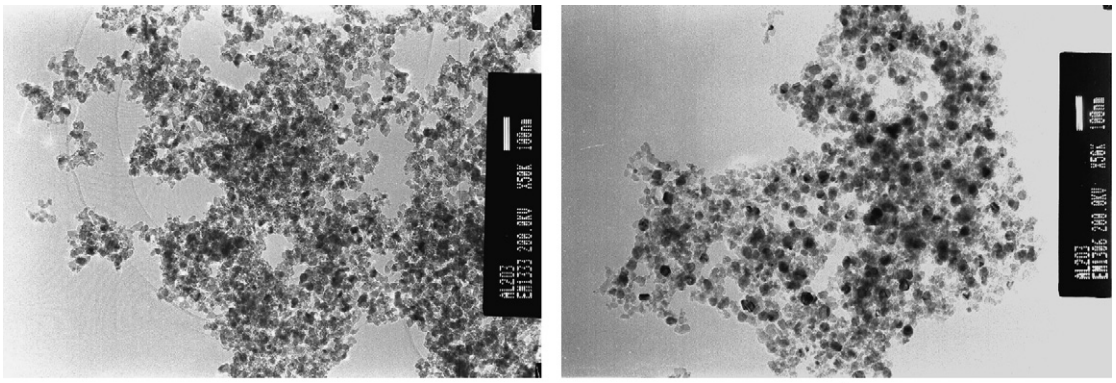

(a) (b)

Fig. 4. TEM micrographs of 15 vol.% Co/Al_2O_3 composite powders (a) the calcined powders and (b) the reduced powders at 950 °C.

$CoAl_2O_4$ are found (Fig. 2). After in situ reduction in H_2 at 950 °C, α-Al_2O_3 and fcc-Co are observed (Fig. 3a). Whereas, the specimens are composed of α-Al_2O_3, fcc-Co and a little amount of hcp-Co after hot-pressing at 1400 °C in Ar under 30 MPa for 30 min (Fig. 3b). The phase transformation of part of cobalt metal took place from high-temperature metastable fcc to low-temperature stable hcp during cooling, thus fcc-Co and hcp-Co normally coexist at room temperature.

Fig. 4a and b are TEM morphological characteristics of Co/Al_2O_3 composite powders after calcination at 850 °C and reduction in H_2 at 950 °C, respectively. It can be seen that the non-agglomerate nanocrystalline co-deposited Co/Al_2O_3 composite powders are detected. The powders reduced at 950 °C contain the homogeneous dispersion of nanometric cobalt particles (about 20–30 nm) in the Al_2O_3 matrix. Compared to the calcined powders, the grain size increases

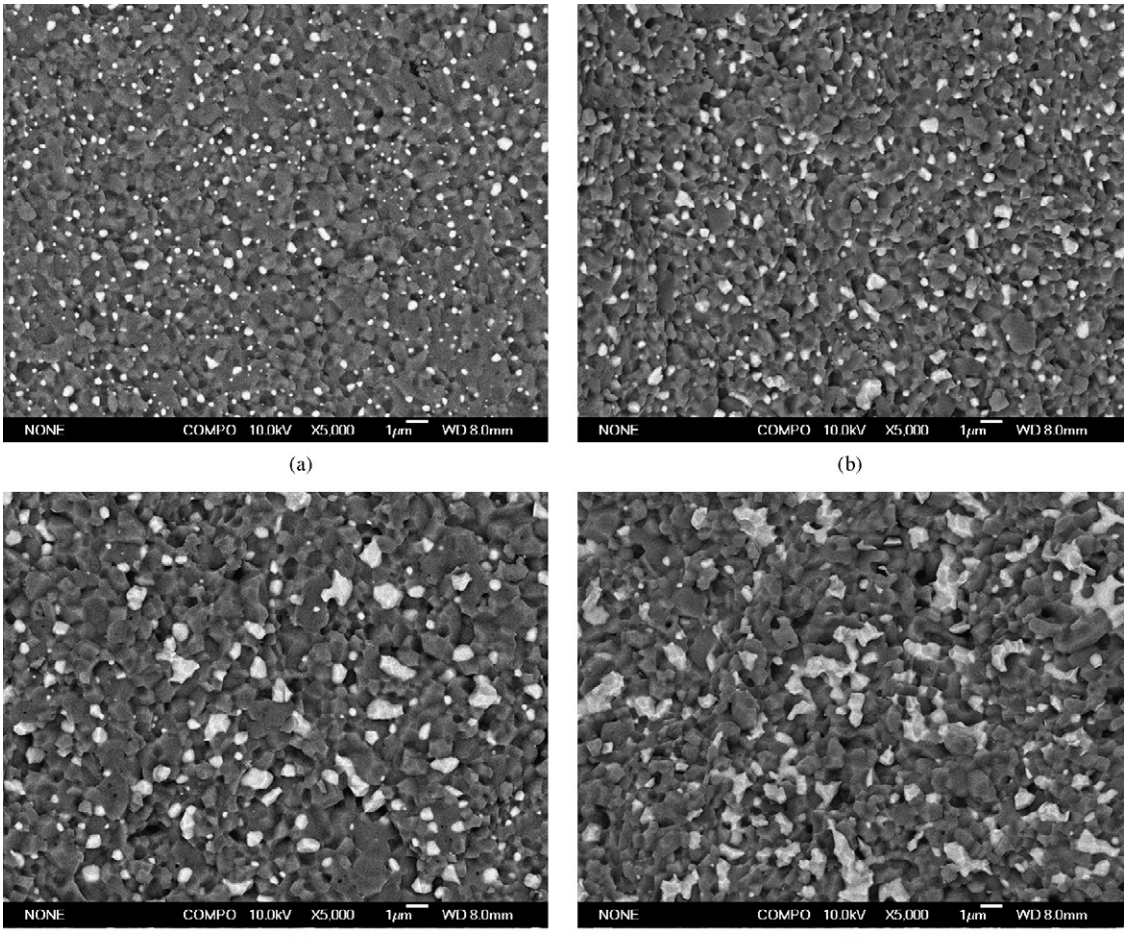

(a) (b) (c) (d)

Fig. 5. SEM micrographs of the fracture surface for Co/Al_2O_3 hot-pressed at 1400 °C for 30 min ((a) AC5, (b) AC10, (c) AC15, (d) AC20; A, Al_2O_3; C, Co).

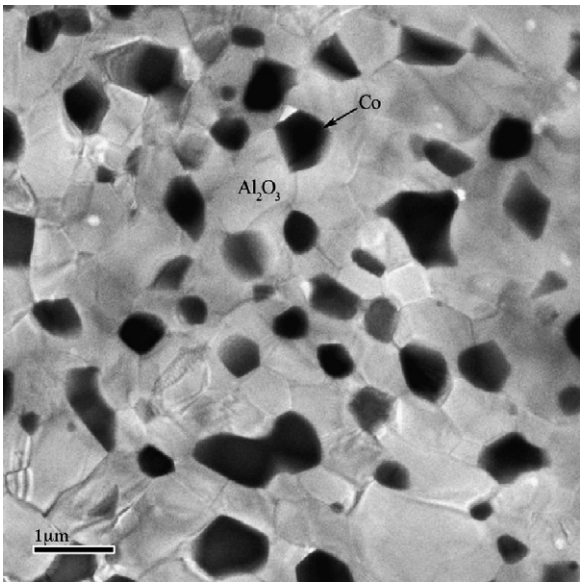

Fig. 6. TEM micrograph for 15 vol.% Co/Al_2O_3 hot-pressed at 1400 °C for 30 min.

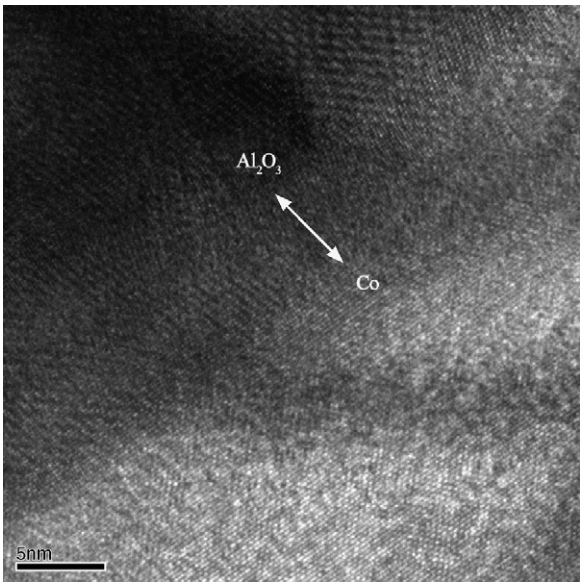

Fig. 7. HRTEM image of the interface between the Al_2O_3 matrix and the cobalt particle.

slightly and there is no change in the morphology and microstructure.

Fig. 5 shows SEM micrographs of the fracture surface for Co/Al_2O_3 hot-pressed at 1400 °C for 30 min in Ar (AC5, AC10, AC15, AC20 mean 5 vol.% Co/Al_2O_3, 10 vol.% Co/Al_2O_3, 15 vol.% Co/Al_2O_3, 20 vol.% Co/Al_2O_3 composites, respectively). The Co phase appears light and the Al_2O_3 matrix dark. The cobalt particles are uniformly dispersed into the Al_2O_3 matrix. At low Co-content, the cobalt particles are dispersed particularly finely and homogeneously along the matrix grain boundaries. With increasing of Co-content, growth as well as coalescence of cobalt particles occurred. The coalescence may have resulted from agglomeration of Co particles due to the addition of much more Co-content. Addition of Co metal suppresses the grain growth and refines the grain size. Nevertheless, the fine particle dispersion of Co metal inhibits the grain-boundary motion of Al_2O_3, leading to an amount of porosity.

Fig. 6 shows TEM images of 15 vol.% Co/Al_2O_3 composites. The submicron size cobalt particles are dispersed at the Al_2O_3 matrix grain boundary. Most of the triple junctions are occupied by Co particles. At the same time, the shrinkage pores are observed because of the difference of the coefficient of thermal expansion (CTE) between Al_2O_3 matrix and Co particles.

The high-resolution transmission electron microscopy (HRTEM) images of the interfaces between the Al_2O_3 matrix and the large cobalt particles are shown in Fig. 7. The interface structure changes in the region thickness of 5 nm, which may serve as a proof of the bonding to some degree between Al_2O_3 and cobalt at the interface.

3.2. Magnetic properties of Co/Al_2O_3 composites

The dependence of magnetization on the applied magnetic field (H) for Co/Al_2O_3 composites is shown in Fig. 8. It exhibits typical ferromagnetic behaviors with hysteresis loop. The susceptibility for Co/Al_2O_3 composites increases with increasing of Co-content. The remanent magnetization (M_r) and saturation magnetization (M_s) increases, whereas the coercive force (H_c) decreases notably as the content of cobalt increases. The remantent magnetization (M_r) and saturation magnetization (M_s) increases with the increasing of Co-content, resulting from the growth of the Co particles. The coercive force (H_c) is well known to be strongly dependent on the grain size, residual stress, and dislocation density [17–19]. The grain size, as shown in Fig. 5, is the main factor. Schematic representation of the change of intrinsic coercivity as a function of the size of the magnetic particles is shown in Fig. 9. Above a critical particle size, D_s, the particles are multi-domain. The coercivity

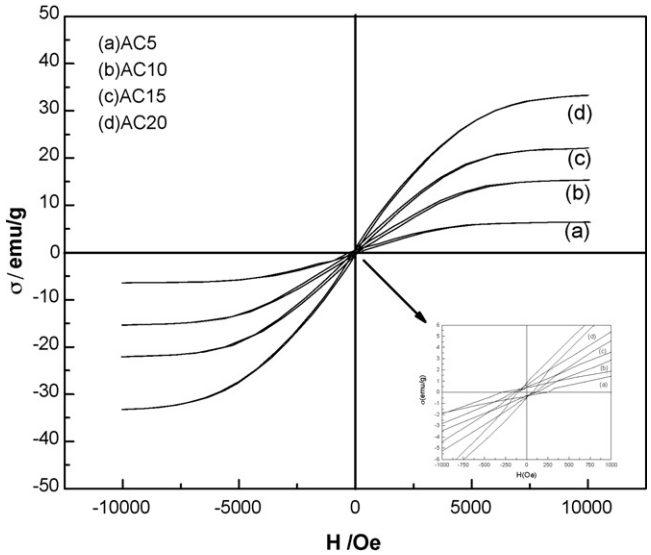

Fig. 8. Room-temperature hysteresis loops for the Co/Al_2O_3 hot-pressed at 1400 °C in Ar for 30 min.

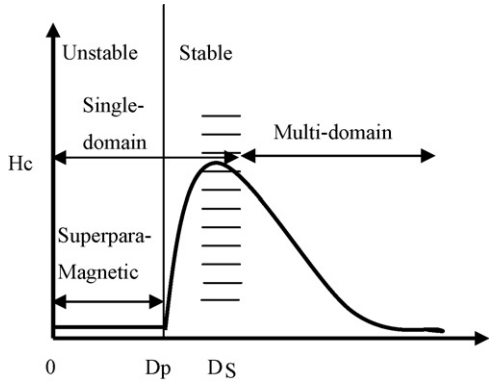

Fig. 9. Schematic representation of the change of intrinsic coercivity as a function of the size of the magnetic particles.

decreases as the particle size increases due to the movement of domain walls. Below D_s, the particles are single-domain, the magnetic moment of the particles will be gradually affected by thermal fluctuation, leading to the decreasing of H_c [20]. As shown in Fig. 8, at lower Co-content, the size of the Co particles is close to D_s and has the high coercivity. With increasing of Co-content, the particle size of the magnetic cobalt is grown and coalesced in the Al_2O_3 matrix to micrometer order, then, leading to the decreasing coercive force (H_c).

In addition, the residual stress is one of important factors on the magnetic properties for Co/Al_2O_3 composites. The residual stresses are mainly induced by the mismatch in CTE of the Al_2O_3 matrix and submicron-sized Co particles. The phase transformations of part of cobalt particles also produce the residual stresses. According to Fig. 3b, only a little amount of hcp-Co existed, so the mismatch in CTEs is the dominant cause. The residual stresses will restrict the spin of magnetic domain wall. According to Kohle et al. [21], the residual stresses σ_{th} at the metal/ceramic interface due to the difference in coefficient of thermal expansion (CTE) can be calculated from:

$$\sigma_{th} = \frac{[(1+\nu_c)^2\alpha_c - (1+\nu_{me})^2\alpha_{me}]\Delta T_s}{((1-2\nu_{me})(1+\nu_{me})/E_{me}) + ((1+2\nu_c)/E_c)},$$

where ν_c and E_c are the Poisson's ratio and Young's modulus of the matrix phase; ν_{me} and E_{me} the Poisson's ratio and Young's modulus of the dispersing phase; α_c and α_{me} the CTEs of matrix phase and dispersing phase, respectively; ΔT_s is the temperature difference between sintering temperature and room temperature. For Co/Al_2O_3 composites, $\nu_{Co} = 0.32$; $\nu_{Al_2O_3} = 0.23$; $E_{Co} = 183$ GPa; $E_{Al_2O_3} = 402$ GPa; $\alpha_{Co} = 12.5 \times 10^{-6}\,K^{-1}$;$\alpha_{Al_2O_3} = 80.6 \times 10^{-6}\,K^{-1}$; $\Delta T_s = 1400\,^{\circ}C$. From Eq. (1), the results show that the stresses at the Co/Al_2O_3 interface are 2.17 GPa. As is shown here, the large residual stresses can lower the energy of the Bloch-walls between domains, and thus make their movement difficult, leading to higher coercive force.

Moreover, the heterogeneous interface, as shown in Fig. 7, resulting from cobalt particles fixed to Al_2O_3 matrices becomes also a pinning site of the movement of the magnetic domain walls. In conclusion, cobalt is uniformly dispersed into Al_2O_3 matrix without losing its ferromagnetic properties in our present work. The grain size and residual stresses are the main factors on the magnetic properties for Co/Al_2O_3 composite ceramics.

4. Conclusions

The present work has shown that high density Co/Al_2O_3 composite ceramics can be fabricated by calcination, reduction and hot-pressing processes to the precursor of Co/Al_2O_3 composite powders prepared by co-deposition method. Microstructural observations revealed that the submicron-sized cobalt particles are uniformly dispersed into Al_2O_3 matrix, located mainly along the matrix grain boundaries. The growth of cobalt particles took place with increasing Co-content. The Co/Al_2O_3 composites exhibited typical ferromagnetic behavior resulting from the ferromagnetism of submicron-sized cobalt. The magnetic properties in Co/Al_2O_3 systems required in practical use can be obtained by tailoring the compositions and fabrication procedures.

Acknowledgements

The authors acknowledge support from National Natural Science Foundation of China (50220160657) and Shanghai Importance Fundamental Project (04DZ14002), as well as the metal matrix composites state key lab of Shanghai Jiaotong University.

References

[1] M. Sternitzke, J. Eur. Ceram. Soc. 17 (1997) 1061–1082.
[2] T. Sekino, T. Nakajima, S. Ueda, K. Niihara, J. Am. Ceram. Soc. 80 (5) (1997) 1139–1148.
[3] S.-T. Oh, T. Sekino, K. Niihara, J. Eur. Ceram. Soc. 18 (1998) 31–37.
[4] W.H. Tuan, R.J. Brook, J. Eur. Ceram. Soc. 6 (1990) 31–37.
[5] S.-C. Wang, C.-J. Wei, Nanostruct. Mater. 10 (6) (1998) 983–1000.
[6] W.P. Tai, T. Watanbe, J. Mater. Sci. 33 (1998) 5795–5801.
[7] W.P. Tai, Y.S. Kim, J.G. Kim, Chem. Phys. 82 (2) (2003) 396–400.
[8] W.H. Tuan, M.C. Lin, H.H. Wu, Ceram. Int. 21 (4) (1995) 221–225.
[9] I. Levin, W.D. Kaplan, D.G. Brandon, A.A. Layyous, J. Am. Ceram. Soc. 78 (1995) 254–256.
[10] O. Aharon, S. Bar-Ziv, D. Gorni, T. Cohen-Hyams, W.D. Kaplan, Scrip. Mater. 50 (9) (2004) 1209–1213.
[11] D.-M. Liu, W.H. Tuan, C.-C. Chiu, Mater. Sci. Eng. B 31 (3) (1995) 287–291.
[12] A. Santos, J.D. Ardisson, A.D.C. Viegas, J.E. Schmid, A.I.C. Persiano, J. Magn. Mater. 226–230 (2001) 1861–1863.
[13] M. Leverkoehne, V.S.R. Murthy, R. Janssen, N. Claussen, J. Eur. Ceram. Soc. 22 (2002) 2149–2153.
[14] M. Pardavi-Horvath, L. Takacs, Source Magn. 28 (5) (1992) 3186–3188.
[15] Y.D. Li, C.W. Li, X.F. Duan, J. China Univ. Sci. Technol. 27 (3) (1997) 346–351.
[16] J.A. Dean, Lang's Handbook of Chemistry, 13th ed., McGraw-Hill Book Company, 1985.
[17] S. Chikazumi, Physics of Ferromagnetism-Magnetic Characteristic and Engineering Applications, first ed., Syokado, Tokyo, Japan, 1984.
[18] L. Daroczi, D.L. Beke, G. Posgay, G.F. Zhou, H. Bakker, Nanostruct. Mater. 2 (5) (1993) 515–525.
[19] R. Kamel, A. Reffat, Solid State Commun. 8 (11) (1970) 821–823.
[20] J.S. Miller, M. Drillon, Magnetism: Molecules to Materials, vol. III, Wiley-VCH Verlag GmbH, 2002, pp. 21–22.
[21] R. Kohle, C.Y. Hui, E. Ustundag, S.L. Sass, Acta Mater. 44 (1) (1996) 279–287.